Irrig Sci
DOI 10.1007/s00271-014-0456-y

REVIEW

Seasonal evolution of crop water stress index in grapevine varieties determined with high-resolution remote sensing thermal imagery

J. Bellvert · J. Marsal · J. Girona · P. J. Zarco-Tejada

Received: 9 June 2014 / Accepted: 27 October 2014

Abstract The seasonal characterization of spatial variability in water requirements across and within vineyards could assist the viticulturist to fine-tune irrigation management for quality optimization. Remotely sensed crop water stress index (CWSI) is related to crop water status, but it is not known how applicable it is to different grape varieties at different times of the season. This study focused on the determination of the lower and upper baselines for calculating CWSI for the Chardonnay, Pinot-noir, Syrah and Tempranillo varieties at different phenological stages. Baselines were determined based on canopy temperatures measured with infrared temperature sensors placed on top of well-watered grapevines in 2011. Results indicated that non-water-stressed baselines differed depending on variety and phenological stage. During 2011, an aircraft equipped with a thermal camera flew over the vineyards on six particular days throughout the season at 150 m altitude above ground level. At the same time, leaf water potential (Ψ_L) was measured for each variety. Variety and phenological stage affected the relationship between remotely sensed CWSI and Ψ_L, with phenology having greater influence on the observed measurements than on variety. For instance, the one-to-one relationship between estimated and measured Ψ_L had R^2 of 0.634 and 0.729 for variety and phenology, respectively. The baselines and estimations of Ψ_L were validated in different vineyards of the same region and in a different season (2013) using the same methodology as in 2011. Data obtained in 2013 were in agreement with observations during 2011. It is concluded that the use of CWSI for assessing vineyard water status requires calibration to account for the effects, primarily of phenological stage, but also, of variety. Once calibrated, this can be successfully applied to other vineyards and seasons.

Communicated by V. Sadras.

J. Bellvert (✉) · J. Marsal · J. Girona
Efficient Use of Water Program, Institut de Recerca i Tecnologia Agroalimentàries (IRTA), Fruitcentre, Parc Cientific i Tecnològic Agroalimentari (PCiTAL), 25003 Lleida, Spain
e-mail: joaquim.bellvert@irta.es

P. J. Zarco-Tejada
Institute for Sustainable Agriculture (IAS), Consejo Superior de Investigaciones Científicas (CSIC), Alameda del Obispo, s/n, 14004 Córdoba, Spain

Introduction

The crop water stress index (CWSI) was developed as a normalized index to quantify stress and overcome the effects of other environmental parameters affecting the relationship between stress and plant temperature (Idso et al. 1981; Jackson et al. 1981). CWSI can be determined by at least three different methodologies. The empirical approach is based on relating canopy–air temperature difference ($T_c - T_a$) to air vapour pressure deficit (VPD) of a ‘non-water-stressed baseline’ (NWSB) referring to a well-watered crop transpiring at the potential rate (maximum stomatal conductance, g_s) (Idso et al. 1981). A second method is based on the energy balance equation and requires an estimate of net radiation and an aerodynamic resistance factor (Jackson et al. 1988). The other alternatives are based on using natural (Clawson et al. 1989; Leinonen and Jones 2004) and artificial (Meron et al. 2003) wet and dry reference surfaces.

The CWSI has been successfully related to leaf water potential (Ψ_L) for different grapevine varieties by using some of these methodologies. Examples have been reported for Pinot-noir using the empirical approach (Bellvert et al.

Published online: 18 December 2014

2014), or for Merlot (Möller et al. 2007) and Cabernet Sauvignon (Weathon et al. 2011) using artificial reference surfaces. However, different criteria used for calculating CWSI prevent comparison between varieties. In addition, all the studies have shown relationships on specific days, but is not known whether the relationship between CWSI and Ψ_L would change during different phenological stages. Remotely sensed CWSI is advantageous for detection of plant water status variability within orchards (Berni et al. 2009a; Bellvert et al. 2014). For CWSI to be a successful tool for detecting plant water status along the season in vineyards, information on the interaction between varieties and phenology in the relationship between CWSI and Ψ_L is needed.

For practical purposes, it is desirable to have a robust relationship between remotely measured CWSI and 'true' ground-based measures of crop water status throughout the season. However, stomatal control over water vapour conductance is highly sensitive to VPD (e.g. Soar et al. 2006a, b; Poni et al. 2009; Rogiers et al. 2012), and there are clear differences in this response between varieties (Schultz and Stoll 2010; Soar et al. 2006b). These differences may affect canopy temperature and its relationship with plant water status. Therefore, the response of stomata to variations in Ψ_L can be different among varieties. Some studies have also reported that stomatal responses to Ψ_L have different sensitivity between different phenological stages (Marsal and Girona 1997 in peach; McCutchan and Shackel 1992 in plum; Olivo et al. 2009 in grapevine). Olivo et al. (2009) reported baselines between variations of Ψ_L and vapour pressure deficit at different phenological stages in Tempranillo grapevines.

Considering that VPD influences stomatal behaviour and therefore canopy temperature, and that VPD varies seasonally, we hypothesize that phenology and variety would influence the determination of the crop water stress baselines in grapevines. The goal of this study was first to determine the non-water-stressed baselines (NWSB) and the CWSI for the four grapevine varieties Pinot-noir, Chardonnay, Syrah and Tempranillo at different phenological stages. Additionally, work to establish the seasonal relationships between CWSI and Ψ_L was carried out by simultaneously measuring Ψ_L and estimating CWSI using remote sensing thermal images.

Materials and methods

Study site

The study was carried out during the 2011 growing season in commercial vineyards of Pinot-noir, Chardonnay, Syrah and Tempranillo located in Raïmat (41°39′N, 00°30′E), Lleida, Spain. The areas of the plots were 11.0, 22.0, 18.4 and 14.5 ha, respectively. The vines were aged 20, 11, 9 and 13 years old, respectively. Vines were planted in a grid of 1.7 m × 3.1 m for Pinot-noir and 2.0 m × 3.0 m for the other varieties, all of them with north–south row orientation. Canopies were cordon-trained to an espalier system at a height of 0.9 m, and their width ranged from 25 to 80 cm. Canopy management practices aimed at producing high-quality grapes by limiting canopy growth and included vertical shoot positioning in July. The climate of the area is Mediterranean, with an average annual rainfall of 291.3 mm. Annual reference evapotranspiration (ET_o) was around an average of 1,080 mm. Irrigation season started in April and lasted until October. Frequency of irrigation applications varied from 3 to 4 days per week. Irrigation water was applied through a drip irrigation system with emitters spaced 0.85 m apart on single drip line per vine row, discharging 3.7 l h^{-1}. In a small area within each vineyard, twelve grapevines were fully irrigated (100 % of ET_o) to measure canopy temperature under non-stress conditions.

Canopy temperature measurements and CWSI

Two infrared temperature sensors (IRTS) (model PC151LT-0; Pyrocouple series, Calex Electronics Limited, Bedfordshire, UK) were installed at the start of the experiment about 1.5 m above two of the well-watered grapevines of each variety. Leaf water potential (Ψ_L) was measured weekly at 12:00 h in these well-watered vines ensuring that values were above the threshold of −0.8 MPa along the season. According to Girona et al. (2006), a threshold of Ψ_L for a well-watered vine would have a linear decrease from around −0.6 MPa, at the beginning of the irrigation season, down to −0.8 MPa by early June. Two fully expanded leaves exposed to direct sunlight were measured from each vine. A Scholander pressure chamber (Soil Moisture Equipment Corp., Santa Barbara, CA, USA) was used following the recommendations of Turner and Long (1980).

Canopy temperature was measured from 10 May until 15 September, except for Syrah and Tempranillo, which finished on 30 August because of the high defoliation caused by mechanical harvesting. Therefore, the postharvest period was only studied in Pinot-noir and Chardonnay. The calibrated IRTS were installed aiming vertically downward (nadir view). The sensors' angular field of view was 15:1 with an accuracy of ±1%. This narrow angular field of view of the sensor was used in grapevines to be sure that the targeted area was pure vegetation. Visual inspection of sensor positioning and consistency with values measured with a hand-held infrared thermometer (fluke 62 mini, Fluke Europe, Eindhoven, Netherlands) ensured that 100 % of the temperature signal came from leaves. Details of this instrumental set-up are described in Sepulcre-Canto et al. (2006). All IRTS were connected to a datalogger (model CR200X; Campbell Scientific, Logan, UK) that recorded temperatures every minute and stored the 15-min averages. Recorded data of well-watered grapevines were used to calculate the baselines of the crop water stress index (CWSI). The empirical CWSI is calculated as (Idso et al. 1981):

$$\mathrm{CWSI} = \frac{(T_c - T_a) - (T_c - T_a)_{\mathrm{LL}}}{(T_c - T_a)_{\mathrm{UL}} - (T_c - T_a)_{\mathrm{LL}}} \quad (1)$$

where $T_c - T_a$ is measured canopy–air temperature difference; $(T_c - T_a)_{\mathrm{LL}}$ lower limit of $(T_c - T_a)$ of a canopy which is transpiring at the potential rate; and $(T_c - T_a)_{\mathrm{UL}}$ expected differential in the case of a non-transpiring canopy.

The methodology described in Bellvert et al. (2014) was used in this analysis. Each point was obtained from half hourly averages of T_c, T_a and VPD from 11:00 to 16:00 h. Only data from clear days (95 % of days) with wind speed below 6 m s^{-1} (at a height of 10 m) were used in the assessment of CWSI. A problem of the empirical method is that in some instances, the values of CWSI could exceed the range of 0.0–1.0 (Yuan et al. 2004). To help solve this problem, in this study, we propose to use a curvilinear model to adjust the 'non-water-stressed baselines' (NWSB), from the relationship between $T_c - T_a$ for well-watered conditions and vapour pressure deficit. The upper limit (UL) was obtained by solving the NWSB curvilinear equation for VPD = 0 and then correcting for vapour pressure differences caused by the difference in $T_c - T_a$ (Idso et al. 1981). The obtained UL followed a linear regression and represents the maximum $T_c - T_a$ values of severely stressed grapes presumably under complete stomatal closure. The high variability of the NWSBs suggested to calculate the $(T_c - T_a)_{\mathrm{LL}}$ taking the minimum values of $T_c - T_a$ for each VPD (Bellvert et al. 2014). The lower limits (LL) were developed for a relatively wide range of VPD (1–5 kPa). Given the observed differences, the NWSBs were separated according to different phenological stages: (1) from anthesis to fruit set (berries at pea size) (Stage I), (2) from fruit set to veraison (Stage II), (3) from veraison until harvest (stage III) and (4) from harvest until 40 days after harvest (postharvest). Air temperature (T_a) and vapour pressure deficit (VPD) were obtained from two portable weather stations (Watchdog 2000; model 2,475 Plant growth, Spectrum Technologies, Inc. Plainfield, Illinois, USA) located on one side of the vineyards.

Airborne campaign

The airborne campaigns were conducted with a thermal camera (FLIR SC655, FLIR Systems, USA) installed on an aircraft (CESSNA C172S EC-JYN). The camera had a resolution of 640 × 480 pixels, equipped with a 13.1 mm optics focal length yielding an angular FOV of 45° and connected to a computer via USB 2.0 protocol. The spectral response was in the range of 7.5–13 μm. The camera radiometric calibration was assessed in the laboratory using a blackbody (model P80P, Land Instruments, Dronfield United Kingdom). In addition, various calibrations were conducted at the time of each flight using surface temperature measurements to improve the conducted calibration. The accuracy of this method is discussed in Berni et al. (2009a, b), who demonstrated an accuracy below 1 K using a similar camera on board an Unmanned Aerial Vehicle (UAV). The flying pattern was carried out for 250 ha, which contained the four studied plots (Fig. 1a). It consisted of twenty longitudinal lines of 1,500 m separated by 70 m. The flights were conducted at 12:00 solar time (14:00 local time) on 9 and 24 June, 7 July, 4 and 28 August and 12 September of 2011 at 150 m above ground level. Unless otherwise specified, all times referred to here are solar times. Air vapour pressure deficit (VPD) on these days ranged from 1.89 to 4.73 kPa. Images obtained had 30-cm spatial resolution enabling the use of pure grapevine–crown pixel and excluding soil, background targets and shadows (Fig. 1b).

Concomitant to each flight, Ψ_L was measured to compare the temperature obtained from aerial thermal imagery with a ground-based stress indicator. Leaf water potential was measured in eighteen grapevines of each variety, with different water status, one measurement on each vine. Grapevines with different water status were selected in different locations within each plot taking into account spatial variability across vineyards. In each measured vine, aluminium paper was used between rows to mark the exact location where Ψ_L was measured and the considered canopy temperature (T_c) pixels (Fig. 1c). Two teams, each equipped with a pressure chamber on a truck, took all the measurements so that they could be performed within 1 h around the time of flying.

Estimation of leaf water potential from CWSI

Crop water stress index (CWSI) was calculated according to Eq. (1) for each variety at different phenological stages using the developed seasonal baselines. Curves were fitted to the empirical relationships between CWSI and Ψ_L in the following three ways: (a) a general relationship from a composite of all available data, (b) relationships for each grapevine variety and (c) relationships for each phenological stage. For the three relationships, CWSI was determined using the baselines developed from our study. Estimation of Ψ_L was based on using these three relationships and its accuracy analysed in comparison with the observed Ψ_L. To determine which of the three forms of relationship had the best fit and prediction, estimated and observed Ψ_L measurements were plotted against each other.

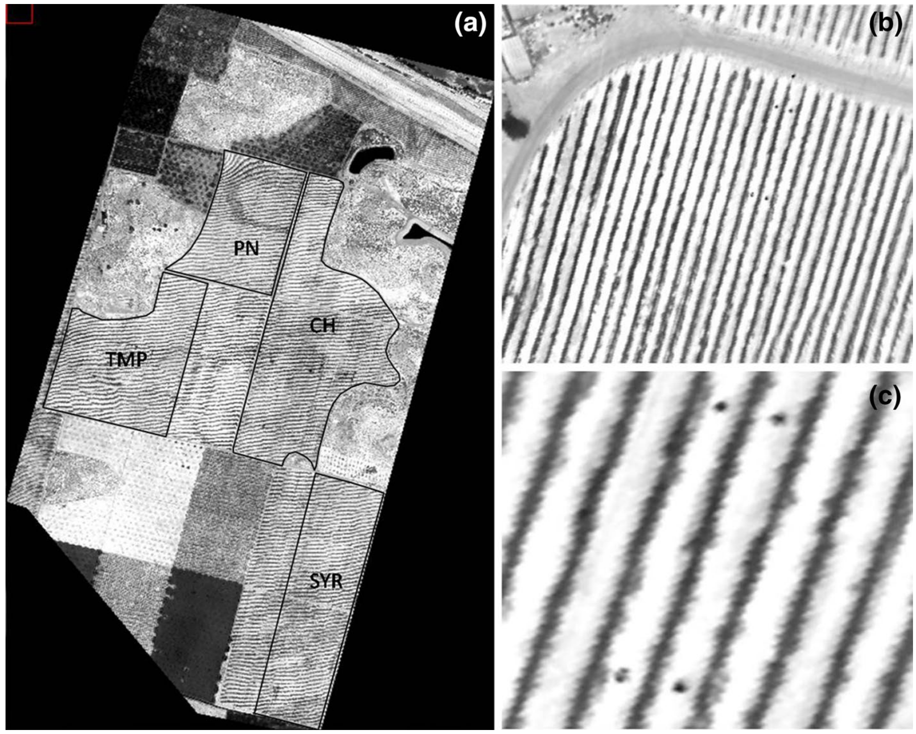

Fig. 1 Thermal mosaic acquired with a FLIR SC-655 thermal camera on board an aircraft yielding 30 cm pixel resolution, observing: **a** the different vineyard plots of Raïmat (Lleida): (1) Pinot-noir (PN), (2) Chardonnay (CH), (3) Tempranillo (TMP) and (4) Syrah (SYR), **b** the vineyard study sites used for field data collection, and **c** detailed image of measured grapevines located with aluminium paper between rows

Image processing methods were used to extract canopy temperature (T_c) from pixels of those vines where Ψ_L was measured. We manually selected the pixels in each vine to ensure that only pure crown vegetative pixels were taken. The same selected pixels in each vine were used to extract T_c in each of the six thermal images.

Validation measurements

The methodology proposed to estimate Ψ_L was validated during 2013 in different vineyards from those of 2011. The new vineyards were located in the same region of Raïmat (Lleida, Spain). Three different vineyards of Chardonnay (13-year old vines) and one of Tempranillo (14-year old vines) were used for the validation. Areas of Chardonnay vineyards were 44.2, 19.0 and 17.8 ha, respectively, and Tempranillo vineyard area was 5.9 ha. The spacing between vines and between rows in Chardonnay vineyards was 2 and 3 m, respectively, and with a north–south orientation. Tempranillo vineyard spacing was 3.2 m between rows and 1.6 m within rows, and with an east–west orientation. Canopies of all vineyards were cordon-trained to an espalier system at a height of 0.9 m, and their width ranged from 25 to 80 cm. All vineyards were under drip irrigation, and irrigation was managed by each grower.

Two and three flights were carried out during stages II and III of each variety, respectively. During each flight, twenty and eight Ψ_L measurements were made, respectively, for each Tempranillo and Chardonnay vineyard. Location of measured vines within each vineyard was randomly selected at each flight. The same methodology described in 2011 for obtaining T_c was also used in 2013. Aluminium paper was also used between rows to mark the exact location where Ψ_L was measured and the considered canopy temperature (T_c) pixels. CWSI of each measured vine was calculated by using the respective phenological baselines developed in this study (Table 3).

Statistical data analysis

Non-watered-stressed baselines (NWSB) were transformed to a linear regression model for the purpose of analysing differences between varieties and phenological stages. A covariance analysis (ANCOVA) was performed to analyse these differences using the SAS statistical package (version 9.2; SAS Institute, Cary, NC, USA). Specific differences among varieties and phenological stages in the slopes and intercept of the lines were subsequently tested by orthogonal contrasts.

Data from the six thermal images were analysed by phenological stages. Stage I corresponded to the thermal image from 9 June (cumulative degree-day since budbreak, CDD = 577). Stage II corresponded to the averaged data obtained on 27 June (CDD = 866) and 8 July (CDD = 1,051). Stage III for Pinot-noir and Syrah was assessed using the averaged data of 4 (CDD = 1,467) and 24 August (CDD = 1,835). Chardonnay was harvested at the beginning of August, and only data of 4

August were used for Stage III. For Tempranillo, we used the averaged data for 4 and 24 August, and 12 September (CDD = 2,144). The postharvest period was studied in Chardonnay and Pinot-noir. Thermal images acquired on 24 August and 12 September referred to 15 and 35 days after harvest for Chardonnay. The 12 September image corresponded to 20 days after Pinot-noir harvest.

Results

Crop water stress index

The calculation of CWSI relies on the relationship between $T_c - T_a$ and VPD of well-watered grapevines to obtain a 'non-water-stressed baseline'. Encompassing all collected data from six grapevine varieties, a significant relationship between $T_c - T_a$ and VPD was detected (Fig. 2). There was, however, a wide range of variability in this relationship, which suggested the need for a separate analysis of data by phenological stage and variety.

The relationships between $T_c - T_a$ and VPD presented a significant phenological response, which mainly indicated differences between stage I and subsequent stages (Figs. 3, 4). Variety also interacted with the seasonal effect. In fact, the covariance analysis performed for each phenological stage indicated a distinctive variety effect with VPD on $T_c - T_a$ (Table 1; Fig. 3). Coefficients of determination (R^2) ranged from 0.401 to 0.667. The slopes of the relationship $T_c - T_a$ versus VPD were significantly different between varieties during stages I and II (Table 1). During stage I in Chardonnay and stage II in Syrah, their slopes were significantly gentler than in other varieties. The variety parameter of the covariance analysis was significant ($P < 0.0001$) during stage III and postharvest stage (Table 1). The varieties that were significantly different during stage III were Chardonnay and Tempranillo. Both varieties had a low intercept during stage III (Fig. 3c), although Tempranillo had the lowest $T_c - T_a$ values in response to VPD in stage III. During the postharvest stage, the intercept of Chardonnay was much lower than that of Pinot-noir. In fact, mean $T_c - T_a$ was −1.62 and −0.03 °C for Chardonnay and Pinot-noir, respectively (Fig. 3d).

Phenological responses in the relationship between $T_c - T_a$ and VPD were analysed for each variety (Fig. 4). The relationship between $T_c - T_a$ and VPD for all seasonal data showed that Pinot-noir and Syrah presented a higher variability in comparison with those of Tempranillo and Syrah. Phenological variations in the $T_c - T_a$ response to VPD for Pinot-noir and Syrah during stage I explained this variability (Fig. 4a, c). In fact, the covariance analysis indicated that the stage parameter (intercept) was significant for varieties Pinot-noir and Syrah (Table 2), and $T_c - T_a$

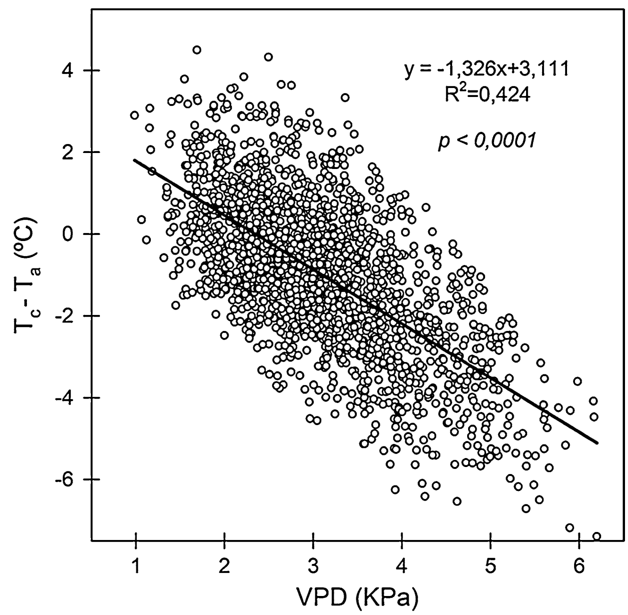

Fig. 2 Relationship between difference of canopy and air temperature ($T_c - T_a$) and vapour pressure deficit (VPD) of all available days of the season in the well-irrigated grapevine varieties of Pinot-noir, Chardonnay, Syrah and Tempranillo. Relationship was obtained using data from 11:00 to 16:00 h

values for both varieties were clearly lower during stage I than those of stages II–III. No significant differences were found in Pinot-noir between stage II–III and postharvest (Fig. 4a). In Chardonnay, the covariance analysis indicated that the interaction between stage and VPD (slope) changed significantly with the phenological stage, with the postharvest stage slope being significantly steeper than that in the pre-harvest stages (Fig. 4b; Table 2). However, non-significant differences were found for the slopes of Chardonnay between stages I and II–III. Phenology did not affect the relationship between $T_c - T_a$ and VPD in well-watered vines of Tempranillo (Fig. 4d; Table 2). The $T_c - T_a$ versus VPD relationships of stages II and III were not significantly different ($P = 0.698$), and data presented in Fig. 4 for both stages were combined to obtain a single baseline (stage II–III).

Equations of the baselines (lower and upper limits, LL and UL) are shown in Table 3. The baselines followed a linear regression model. During stage I, Chardonnay had the maximum intercept of the upper limit (UL) reaching 6.61 °C when vapour pressure deficit was zero (Fig. 5a). At this stage, the upper limits of Pinot-noir and Syrah were similar, but Tempranillo had the lowest intercept. The UL during stages II–III also showed differences between varieties (Fig. 5b). Chardonnay had the maximum intercept, reaching 6.45 °C when vapour pressure was zero. Syrah was the variety that had a UL with the lowest $T_c - T_a$ values. Tempranillo and Pinot-noir had similar ULs during stages II–III. Postharvest

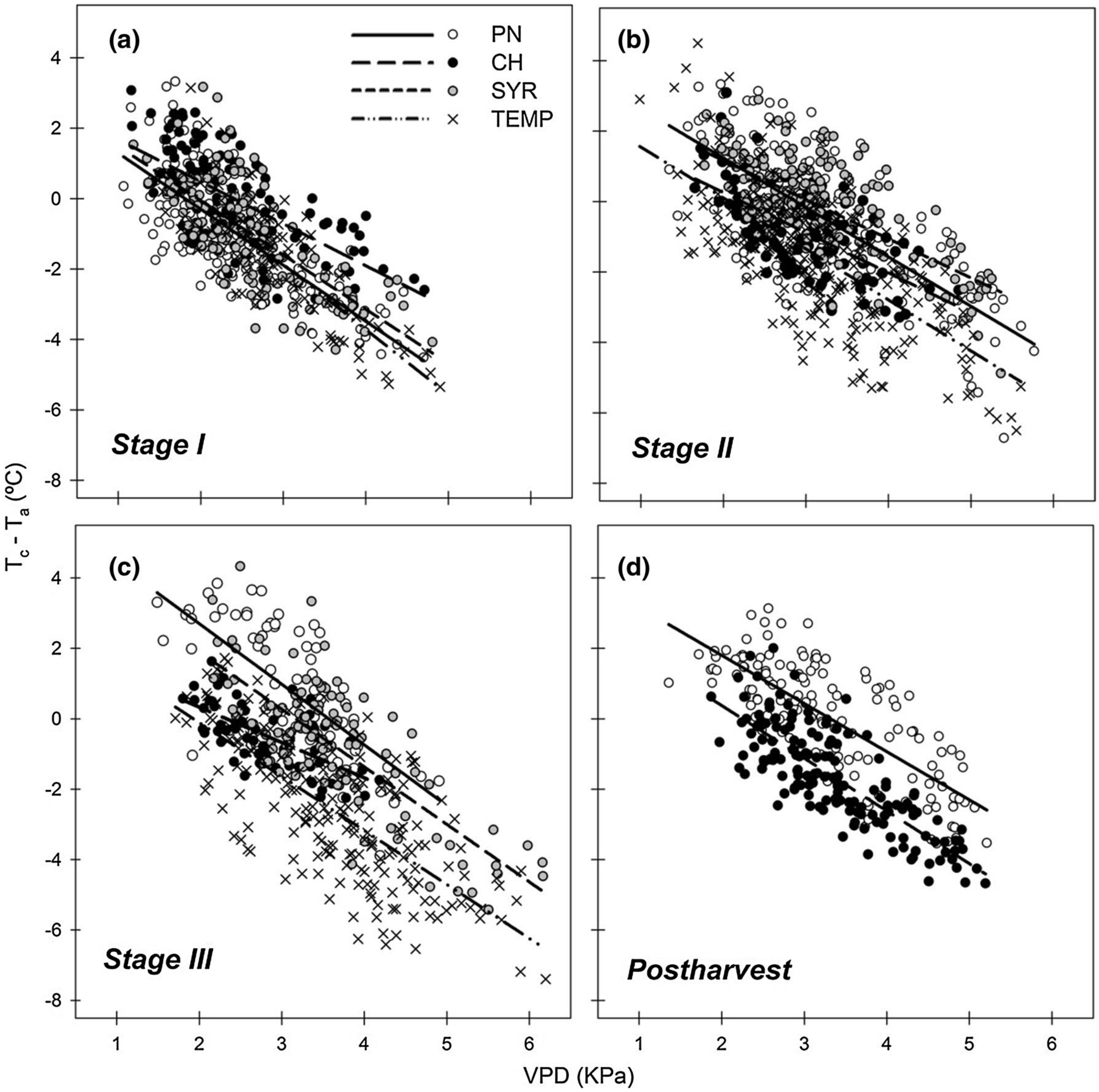

Fig. 3 Differences between varieties Pinot-noir (PN), Chardonnay (CH), Syrah (SYR) and Tempranillo (TMP) in the relationship between difference of canopy and air temperature ($T_c - T_a$) and vapour pressure deficit (VPD) at different phenological stages (Stages I, II, III and postharvest). Equations and coefficients of determination (R^2) are: Stage I; PN: $y = -1.592x + 2.885$, $R^2 = 0.553$; CH: $y = -1.194x + 2.869$, $R^2 = 0.437$; SYR: $y = -1.542x + 3.027$, $R^2 = 0.521$; TMP: $y = -1.848x + 3.675$, $R^2 = 0.649$. Stage II; PN: $y = -1.403x + 4.043$, $R^2 = 0.524$; CH: $y = -1.138x + 2.529$, $R^2 = 0.401$; SYR: $y = -1.026x + 3.066$, $R^2 = 0.457$; TMP: $y = -1.479x + 3.107$, $R^2 = 0.489$. Stage III; PN: $y = -1.722x + 6.146$, $R^2 = 0.469$; CH: $y = -1.004x + 2.335$, $R^2 = 0.426$; SYR: $y = -1.576x + 4.929$, $R^2 = 0.565$; TMP: $y = -1.449x + 2.685$, $R^2 = 0.515$. Postharvest; PN: $y = -1.367x + 4.536$, $R^2 = 0.575$; CH: $y = -1.540x + 3.535$, $R^2 = 0.667$. All relationships were significant ($P < 0.0001$)

period showed differences in the baselines between Pinot-noir and Chardonnay (Fig. 5c). The maximum intercept of the UL corresponded to Pinot-noir, reaching 5.38 °C when vapour pressure deficit was zero. Analysing differences between the baselines among phenological stages, it seems that the UL did not vary between stage I and II–III, with the exception of Tempranillo, which had a higher intercept during stages II–III than in stage I. During postharvest, the UL of Chardonnay appeared with a downward shift compared with pre-harvest stages. The lower limits (LL) showed that during stages II–III, Tempranillo was the variety that displayed more transpirational cooling for a given increase in the air vapour pressure deficit. During postharvest, the LL of Chardonnay had a slope and intercept lower than Pinot-noir.

Relationships between remotely sensed CWSI and midday Ψ_L

Midday Ψ_L measurements correlated significantly with remotely sensed CWSI for our four varieties (Fig. 6).

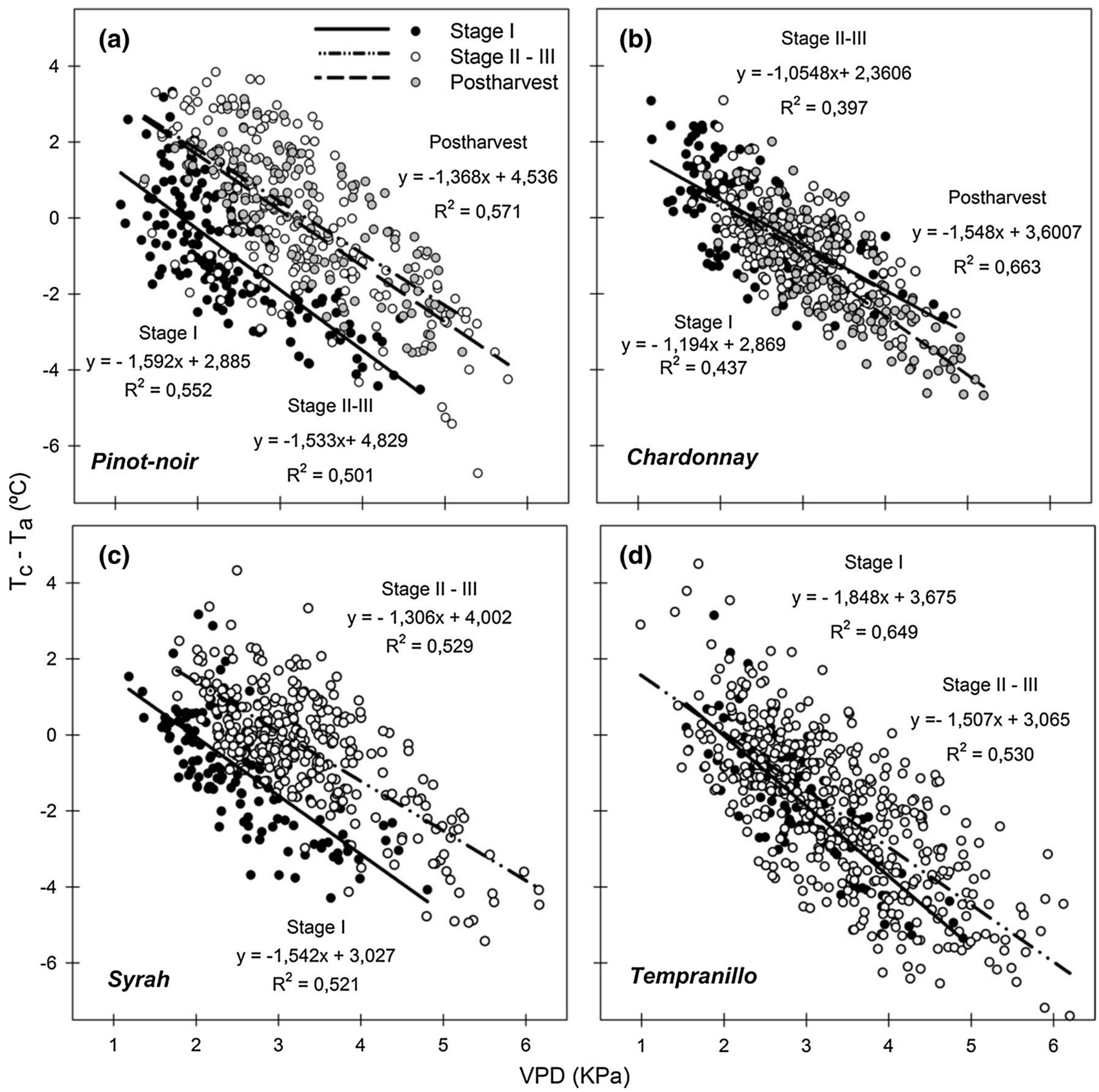

Fig. 4 Seasonal response of difference between canopy and air temperature ($T_c - T_a$) to vapour pressure deficit (VPD) for Pinot-noir (PN), Chardonnay (CH), Syrah (SYR) and Tempranillo (TMP). Regression lines are plotted for each phenological stage. Data from stages II and III were combined in this analysis to obtain a single baseline of stage II–III. All relationships were significant ($P < 0.0001$)

However, the relationship found when using all data indicated a high variability (Fig. 6a), which suggested the need for separate data analysis by variety and phenological stage.

All relationships followed a curvilinear model, indicating the existence of a threshold of CWSI before Ψ_L started to decline significantly. Maximum CWSI corresponded to Ψ_L values around −1.6 MPa, with the exception of Tempranillo which seemed to be around −1.4 MPa (Fig. 6b). This point was associated with complete stomatal closure and zero transpiration. Sensitivity of CWSI to changes in Ψ_L was different between varieties. In Chardonnay, for a given decrease of Ψ_L, changes in CWSI were lower than in the other three varieties. On the contrary, it seems that Tempranillo was the variety which presented the highest changes of CWSI with Ψ_L variations. Phenological effects were also evident; it seems that for a particular level of CWSI, the values of Ψ_L were more negative as the crop developed (Fig. 6c). It seems that the postharvest period was similar to stage III.

These results suggest both a different varietal and seasonal response in the relationship between CWSI and Ψ_L. In order to identify which of the effects had the strongest influence on CWSI versus Ψ_L, Ψ_L was estimated in three different ways and related to observed Ψ_L by linear regression. Ψ_L was first estimated from a general relationship

Table 1 ANCOVA analysis of $T_c - T_a$ for grapevine varieties at different phenological stages and probabilities tested by orthogonal contrasts of slopes (VPD × variety) and intercepts (variety)

ANCOVA	Stage I	Stage II	Stage III	Postharvest
VPD	0.0001*	0.0001*	0.0001*	0.0001*
Variety	0.4203	0.1368	0.0001*	0.0120*
VPD × variety	0.0073*	0.0034*	0.1180	0.3415
Contrast	VPD × variety		Variety	
	Stage I	Stage II	Stage III	Postharvest
CH versus PN	0.0310*	0.2831	0.0003*	0.0122*
PN versus SYR	0.8991	0.0192*	0.1408	–
PN versus TEMP	0.1122	0.2991	0.0001*	–
CH versus SYR	0.0562	0.5592	0.0065*	–
CH versus TEMP	0.0010*	0.0690	0.9999	–
SYR versus TEMP	0.1094	0.0004*	0.0001*	–

* Significant at $P < 0.05$ (SAS 2002)

Table 2 ANCOVA analysis of $T_c - T_a$ for phenological stages and probabilities tested by orthogonal contrasts of slopes (VPD × stage) and intercepts (stage)

ANCOVA	Chardonnay	Pinot-noir	Syrah	Tempranillo
VPD	0.0001*	0.0001*	0.0001*	0.0001*
Stage	0.0551	0.0003*	0.0192*	0.2855
VPD × stage	0.0037*	0.4543	0.1055	0.0657
Contrast	VPD × stage	Stage		
	Chardonnay	Pinot-noir	Syrah	
I versus II–III	0.5723	0.0002*	0.019*	–
I versus PH	0.0142*	0.0021*	–	–
II–III versus PH	0.0018*	0.9284	–	–

* Significant at $P < 0.05$ (SAS 2002)

Table 3 Equations of lower and upper limits for each phenological stage of the grapevine varieties Pinot-noir, Chardonnay, Syrah and Tempranillo

	Lower limits			Upper limits		
	Stage I	Stage II–III	Postharvest	Stage I	Stage II–III	Postharvest
Pinot-noir	$y = -1.544x + 1.226$	$y = -1.331x + 1.332$	$y = -1.593x + 3.887$	$y = 0.429x + 5.043$	$y = 0.316x + 5.808$	$y = 0.250x + 5.383$
Chardonnay	$y = -2.226x + 3.638$	$y = -1.393x + 2.157$	$y = -1.285x + 1.551$	$y = 0.632x + 6.609$	$y = 0.635x + 6.451$	$y = 0.205x + 4.415$
Syrah	$y = -2.213x + 3.176$	$y = -1.465x + 2.729$	–	$y = 0.371x + 4.653$	$y = 0.228x + 4.673$	–
Tempranillo	$y = -1.438x + 1.098$	$y = -1.780x + 1.253$	–	$y = 0.261x + 3.977$	$y = 0.466x + 5.317$	–

y corresponds to difference of canopy and air temperature ($T_c - T_a$), and x represents vapour pressure deficit (VPD)

between CWSI and observed Ψ_L, and subsequently for each varietal and phenological relationship. The one-to-one relationships between estimated and observed Ψ_L were significant ($P < 0.0001$), but differences in their slopes and intercepts were found depending on the method used for estimating Ψ_L (Fig. 7). The linear regression from a general relationship showed the lowest coefficient of determination (R^2) (Fig. 7a). This regression also had the lowest slope and intercept. The linear regression for estimating Ψ_L when considering variety had a higher R^2 than the general estimation (Fig. 7b). The slope and intercept of the regression were also higher in comparison with the general estimation.

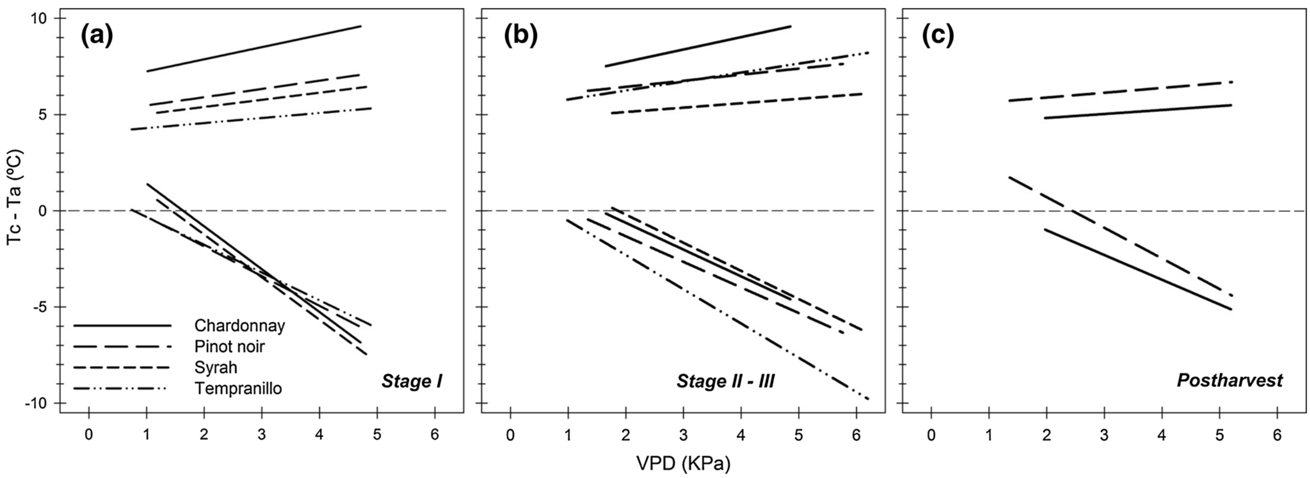

Fig. 5 Lower and upper limits of the relationships between ($T_c - T_a$) and VPD for determination of crop water stress index (CWSI) in Chardonnay, Pinot-noir, Syrah and Tempranillo, at phenological stages: **a** Stage I, **b** Stage II–III and **c** Postharvest. Equations are shown in Table 3

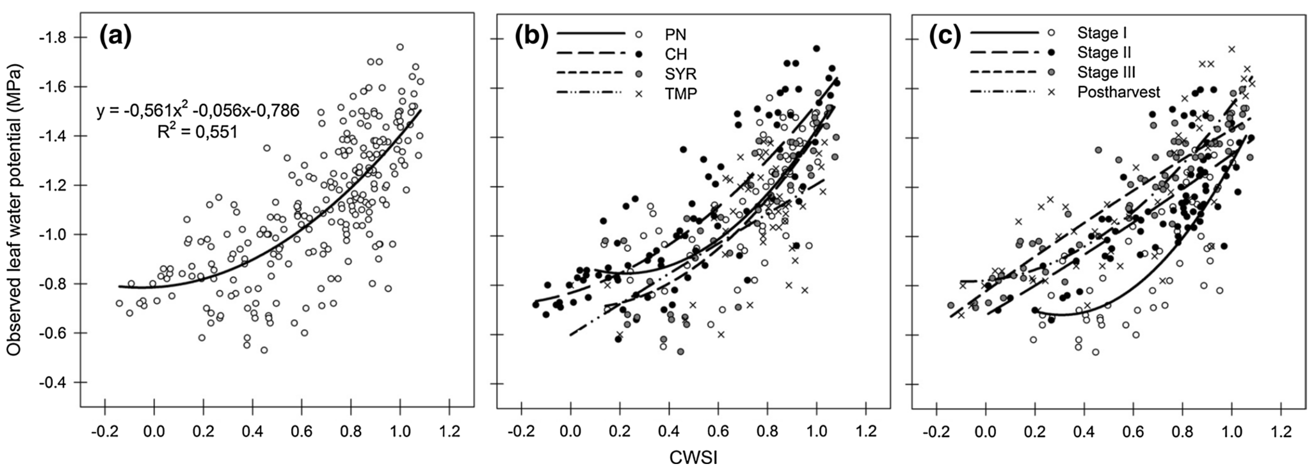

Fig. 6 Relationships between CWSI and observed leaf water potential (Ψ_L), showing in: **a** a general relationship with all data, **b** relationships for grapevine varieties and **c** relationships for phenological stages. Equations and coefficients of determination (R^2) of the relationships shown in b and c were: **b** PN: $y = -0.963x^2 + 0.425x-0.895$, $R^2 = 0.571$, CH: $y = -0.464x^2-0.303x-0.769$, $R^2 = 0.724$, SYR: $y = -0.762x^2 + 0.058x-0.709$, $R^2 = 0.752$, TMP: $y = 0.016x^2-0.628x-0.598$, $R^2 = 0.561$. **c** Stage I: $y = -1.294x^2 + 0.798x-0.805$, $R^2 = 0.647$, Stage II: $y = -0.063x^2-0.589x-0.681$, $R^2 = 0.605$, Stage III: $y = 0.061x^2-0.718x-0.778$, $R^2 = 0.861$, Postharvest: $y = -0.616x^2-0.096x-0.821$, $R^2 = 0.715$

Finally, it seems that the best fit was obtained when each phenological stage was considered (Fig. 7c). This relationship presented the highest R^2 and an equation with the closest slope to one and intercept to zero.

Discussion

The developed non-water-stressed baselines and the relationships between CWSI and leaf water potential (Ψ_L) differed with respect to variety and phenological stage. Accordingly, we will discuss first the CWSI baselines and their relationships with Ψ_L, and subsequently the effect of variety and phenological stage.

Crop water stress index baselines

For the four studied varieties, $T_c - T_a$ values for well-watered grapevines decreased as vapour pressure deficit increased (Figs. 3, 4). However, differences in the slopes and intercepts of the relationship between $T_c - T_a$ and VPD were found between varieties and phenological stages. For instance, in stage I of Chardonnay and stage II of Syrah, the relationships presented a gentler slope in comparison

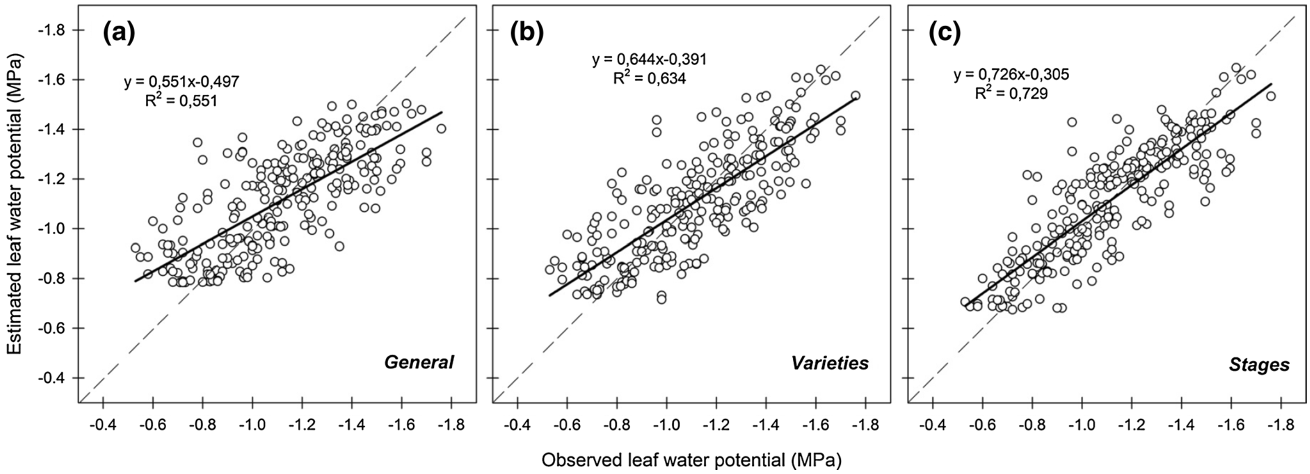

Fig. 7 Simulation of the relationships between observed and estimated Ψ_L, where the latter was calculated from: **a** the general relationship between CWSI and Ψ_L, **b** the relationships between CWSI and Ψ_L for each variety, and **c** the relationships between CWSI and Ψ_L for each phenological stage

with the other varieties (Table 1). This implied that, for a given increase in VPD, Tempranillo and Pinot-noir had more transpirational cooling than Chardonnay and Syrah in their respective stages. The intercept of the $T_c - T_a$ versus VPD relationship was lowest for Tempranillo during stage III, indicating a higher evaporative cooling than Syrah and Pinot-noir (Fig. 3c). Stomatal density, size of stomata and the degree of opening of the pore could modulate stomatal conductance (Weyers and Meidner 1990). Costa et al. (2012) reported a higher leaf stomatal conductance (g_s) and stomatal density in Tempranillo than in Syrah, which could explain, in part, the lower $T_c - T_a$ values found in Tempranillo. Chardonnay was harvested around 15 days before Pinot-noir. So, most of the T_c data measured in Chardonnay during this period corresponded to leaves 15 days younger than those of Pinot-noir, so they could have had a higher transpiration capacity. It should be noted that stage III was longer for the two red varieties (Syrah and Tempranillo) and this could have provided better opportunities for finding differences between the red varieties. Significant differences found in the intercept of Chardonnay and Pinot-noir during postharvest could be related to a leaf age effect (Field 1987).

Different phenological responses in the relationship between $T_c - T_a$ and VPD are also shown in Fig. 4 for some grapevine varieties. Differences between phenological stages may be explained in part by the energy balance of a crop canopy, zenith solar angle or leaf orientation. The intercept of the relationship between $T_c - T_a$ and VPD is a function of aerodynamic resistance to water vapour transfer (r_a) and net radiation (R_n), according to the theoretical equation provided by Jackson et al. (1981). Thus, the intercept is expected to increase with solar radiation. Testi et al. (2008) demonstrated that the intercept of the relationship between $T_c - T_a$ and VPD for well-watered pistachio trees (NWSB) increases with zenith solar angle and probably acts on the targeted canopy temperature area by changing the fraction of shaded leaves. For this reason, as the season advanced, we identified a shift in the intercept of the relationship between $T_c - T_a$ and VPD in Pinot-noir and Syrah (Fig. 4; Table 2). In these two varieties, the intercept increased as the crop developed. This could be explained by assuming that during early stages, both R_n and zenith solar angle are lower. However, this phenological shift was not detected in Chardonnay and Tempranillo, and the reason for this is unknown. The linear relationship between $T_c - T_a$ versus VPD in Pinot-noir was also reported by Bellvert et al. (2014) for 2 years previous to the present study, corresponding to $T_c - T_a = -1.925$ VPD $+ 4.738$. This equation fitted well the relationship of stage II–III from our study (Fig. 4). Despite slight differences in the slopes, the intercepts of both were very similar ($T_c - T_a = -1.533x + 4.829$). This agreement gives consistency to the CWSI approach.

The developed baselines indicate that Chardonnay was the variety that was able to reach the highest leaf temperatures in the UL during pre-harvest stages (Table 3; Fig. 4). Morphological considerations of leaves and canopy light distribution effects may explain part of the leaf heating differences between varieties at stomatal closure. When stomata are closed, leaf temperature becomes more dependent on the ability of a leaf to exchange sensible heat with the air. The heat exchange ability depends in part on the width of the leaf, related to boundary layer development (Gates and Papian 1971; Nobel 2009). Entire leaves, such as those of Chardonnay, may have limited sensible heat exchange and heat up significantly when stomata close in sunny conditions. Moreover, the studied Chardonnay vines had very thin vertical canopies. The compression of large entire flat leaves with high radiative heat loads may have contributed to leaf heating. In contrast, the deeply lobed leaves of Tempranillo and Syrah contained more canopy gaps, which could have produced a wider range of light penetration within the canopy due to a more porous exterior canopy. More radiation penetrating into less exposed leaves may have reduced the intensity of radiation and leaf heating in the more exposed leaves. Pinot-noir leaves tend to be smaller than the others, and probably leaf heating in relation to stomatal closure could be less than in Chardonnay.

Relationship between CWSI and leaf water potential

The established method for quantifying plant water status in grapevines is the measurement of leaf water potential (Ψ_L) (Williams and Araujo 2002). In our work, the relationship between Ψ_L and CWSI had a curvilinear shape and indicated that the transpiration rate must have fallen progressively from a specific Ψ_L threshold until reaching complete stomatal closure (CWSI = 1) (Fig. 6). The high variability found in this relationship when using all data (Fig. 6a) suggested that there might be varietal and/or seasonal effects. Stomatal conductance is the physiological parameter that affects leaf water vapour exchange and therefore canopy temperature. Osmotic adjustment can influence stomatal closure in response to water deficits, as has been shown to occur in the grapevine and to be different among varieties (Costa et al. 2012) and phenological stages (Alsina et al. 2007).

Analysing the relationships among varieties, it seems that different responses in the relationship between Ψ_L and CWSI could be related to their different ability to regulate stomatal aperture. Changes in CWSI were less per unit change of Ψ_L in Chardonnay in comparison with the other three varieties (Fig. 6b). By contrast, Tempranillo had the greatest change in CWSI per unit change of Ψ_L. Chardonnay is characterized by a lower control over stomatal closure under water stress (Schultz 2003; Pou et al. 2012). This may explain the reason why Chardonnay had lower CWSI values in comparison with the other varieties. While vine water status can regulate stomatal conductance, stomatal control over transpiration also involves chemical and/or hydraulic messages (Tardieu and Davies 1993). Thus, differences in hydraulic conductance between varieties may be also related to Ψ_L responses to CWSI. Considerations about this aspect may deserve more attention in further studies. Phenological responses detected in the relationship between CWSI and Ψ_L may depend on osmotic potential and leaf turgor seasonal changes (Fig. 6c). These changes must be associated with fluctuations in leaf transpiration. Alsina et al. (2007) reported differences between varieties and phenological stages in osmotic potential values at full turgor and at the turgor loss point. In most cases, osmotic potential decreased as the crop developed. Girona et al. (2006) also reported in Pinot-noir that Ψ_L values indicative of stress were higher during stage I than in subsequent stages. Therefore, this hypothesis could explain the seasonal relationships shown in Fig. 6c, where for a specific CWSI value, midday Ψ_L was higher at early stages than at full development.

According to these results, it seems that the parameters of both variety and phenology affected the relationship between Ψ_L and CWSI. In fact, the high variability of the general relationship between observed and estimated Ψ_L (Fig. 7a) also indicated that variety and/or phenological stage should be taken into account. Although the consideration of each variety relationship revealed a slight improvement of R^2, slope and intercept of the linear regression of Ψ_L versus CWSI (Fig. 7b), it seems that phenology was the parameter that most affected the relationship between CWSI and Ψ_L (Fig. 7c). To carry out a successful irrigation schedule based on CWSI, we recommend taking into account the differences due to phenological stage as well as the specific influence of Ψ_L for each variety.

Validation measurements

The robustness of the developed seasonal baselines in 2011 for calculating CWSI was tested by evaluating their accuracy on a validation data set during 2013. Estimated CWSI values in 2013 agreed with those of 2011 that were significantly related to Ψ_L for both Chardonnay and Tempranillo (Fig. 8). In agreement with Fig. 6c, the intercept of the relationship CWSI versus Ψ_L was lower in stage II than in stage III. Although in 2013 all Ψ_L values for Tempranillo during stage II indicated that vines were well-watered, this follows the same trend as data from 2011 (Fig. 8a). The data for two different seasons and different vineyards confirmed that the developed seasonal baselines could be implemented in different years for irrigation management purposes. However, it is known that the empirical approach to determine CWSI has some degree of site specificity (Hipps et al. 1985). Thus, the extrapolation of our results to other growing conditions should be performed with caution.

CWSI baselines for this study fitted well for each variety and correlated well with Ψ_L. The results in Pinot-noir were consistent with those developed in previous studies for the same variety. Our results demonstrated the need to develop seasonal baselines for each of the four varieties studied to reduce uncertainty in the calculation of CWSI. The developed baselines (lower and upper limits) showed significant differences among phenological stage and varieties. We suggest that for efficient monitoring of the CWSI, the most

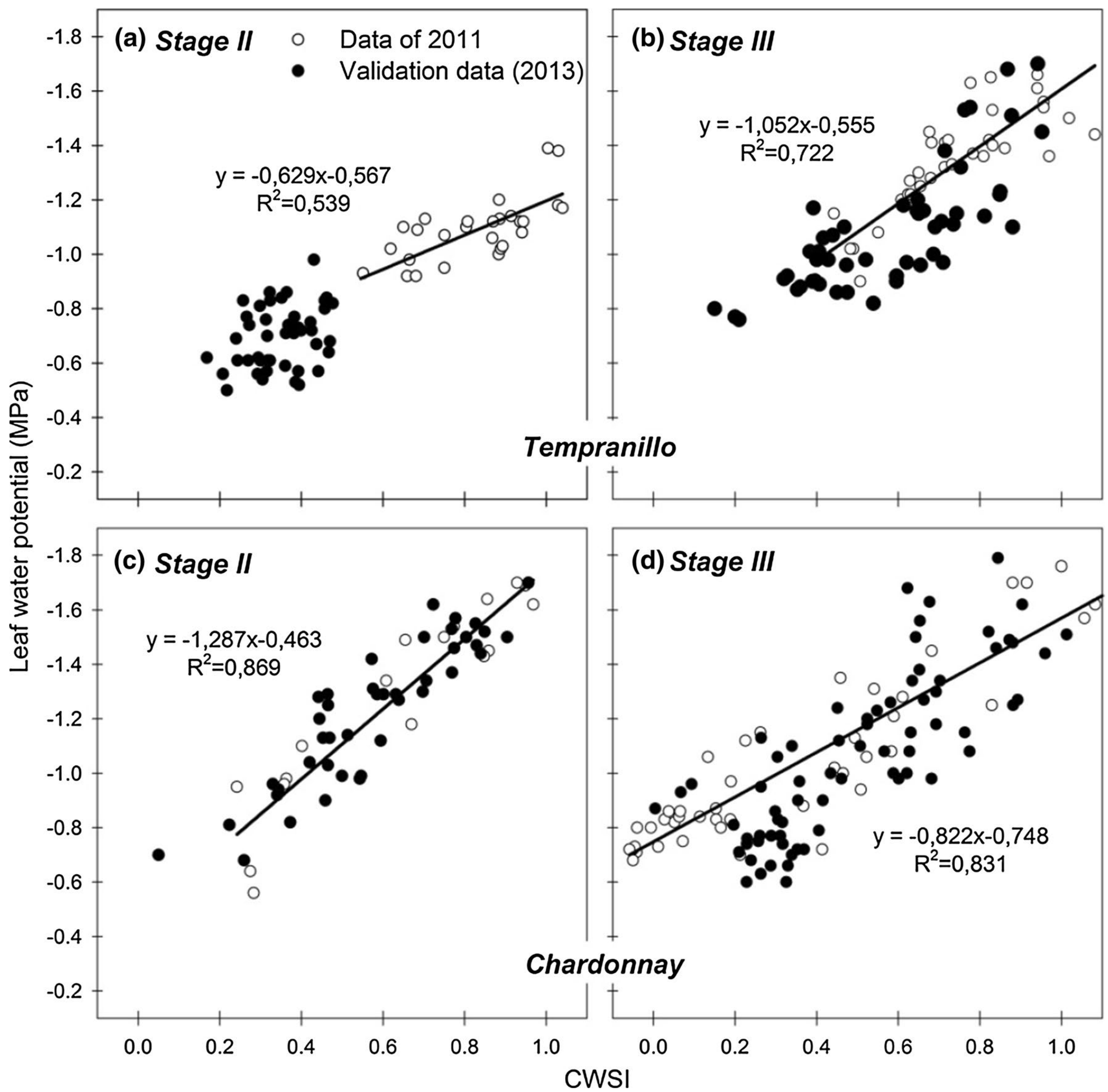

Fig. 8 Validation of the relationships between CWSI and observed leaf water potential (Ψ_L) for varieties Chardonnay and Tempranillo. Validations were obtained separately for the phenological stage II (**a**, **c**) and stage III (**b**, **d**). Relationships corresponded to data obtained during 2011 (*circle*), and validation was made with data from 2013 (*filled circle*). All relationships were significant ($P < 0.0001$)

appropriate procedure would be to establish the baselines and relationships with Ψ_L taking into account first the effect of phenology and secondly the variety.

Acknowledgments The authors thank the team of Quantalab, IAS-CSIC of Córdoba for the technical support in field airborne flights and image processing, and particularly Prof. Elías Fereres, for his comments and suggestions for improving the manuscript. Alberto Hornero, Rafael Romero, David Notario, Alberto Vera, Jaume Casadesús, Xavier Vallverdú and Victoria González-Dugo are especially acknowledged for their technical support with data analysis and useful comments on the manuscript. Mercè Mata, Carles Paris, Jordi Oliver, Gerard Piñol, Núria Bonastre and Núria Civit are acknowledged for field measurements. This work received partial financial support from SUDOE for the European project Telerieg SOE1/P2/E082 and the Spanish Ministry of Science and Innovation (MINECO) for the project CONSOLIDER CSD2006-00067 and AGL2009-13105. We are grateful for the opportunity to carry out this study under the research agreement between CODORNIU and IRTA.

References

Alsina MM, de Herralde F, Aranda X, Savé R, Biel C (2007) Water relations and vulnerability to embolism are not related: experiments with eight grapevine cultivars. Vitis 46(1):1–6

Bellvert J, Zarco-Tejada PJ, Girona J, Fereres E (2014) Mapping crop water stress index in a `Pinot-noir´ vineyard: comparing ground measurements with thermal remote sensing imagery from an unmanned aerial vehicle. Precis Agric 15:361–376

Berni JJ, Zarco-Tejada PJ, Sepulcre-Cantó G, Fereres E, Villalobos F (2009a) Mapping canopy conductance and CWSI in olive orchards using high resolution thermal remote sensing imagery. Remote Sens Environ 113:2380–2388

Berni JA, Zarco-Tejada PJ, Suarez L, Fereres E (2009b) Thermal and narrow-band multispectral remote sensing for vegetation monitoring from an unmanned aerial vehicle. IEEE Trans Geosci Remote Sens 47:722–738

Clawson KL, Jackson RD, Pinter PJ (1989) Evaluating plant water stress with canopy temperature differences. Agron J 81:858–863

Costa JM, Ortuño MF, Lopes CM, Chaves MM (2012) Grapevine varieties exhibiting differences in stomatal response to water deficit. CSIRO publishing. Funct Plant Biol 39(3):179–189

Field CB (1987) Leaf-age effects on stomatal conductance. In: Zeiger E, Farquhar GD, Cowan IR (eds) Stomatal function. Stanford University Press, Stanford, pp 367–384

Gates DM, Papian LE (1971) Atlas of energy budgets of plant leaves. Academic Press, New York

Girona J, Mata M, del Campo J, Arbonés A, Bartra E, Marsal J (2006) The use of midday leaf water potential for scheduling deficit irrigation in vineyards. Irrig Sci 24:115–127

Hipps L, Asrar G, Kanemasu E (1985) A theoretically-based normalization of environmental effects on foliage temperature. Agric For Meteorol 35:113–122

Idso SB, Jackson RD, Pinter PJ, Reginato RJ, Hatfield JL (1981) Normalizing the stress-degree day parameter for environmental variability. Agric Meteorol 24:45–55

Jackson RD, Idso SB, Reginato R, Pinter PJ (1981) Canopy temperature as a drought stress indicator. Water Resour Res 17:1133–1138

Jackson RD, Kustas WP, Choudhury BJ (1988) A re-examination of the crop water stress index. Irrig Sci 9:309–317

Leinonen I, Jones HG (2004) Combining thermal and visible imagery for estimating canopy temperature and identifying plant stress. J Exp Bot 55(401):1231–1243

Marsal J, Girona J (1997) Relationship between leaf water potential and gas exchange activity at different phenological stages and fruit loads in peach trees. J Am Soc Hortic Sci 122(3):415–421

McCutchan H, Shackel K (1992) Stem-water potential as a sensitive indicator of water stress in prune trees (*Prunus domestica* L. cv. French). J Am Soc Hortic Sci 117(4):607–611

Meron M, Tsipris J, Charitt D (2003) Remote mapping crop water status to assess spatial variability of crop stress. In: Stafford J, Werner A (eds) Precision agriculture. Proceedings of the 4th European conference on precision agriculture. Academic Publishers, Berlin, pp 405–410

Möller M, Alchanatis V, Cohen Y, Meron M, Tsipris J, Naor A, Ostrovsky V, Sprintsin M, Cohen S (2007) Use of thermal and visible imagery for estimating crop water status of irrigated grapevine. J Exp Bot 58(4):827–838

Nobel PS (2009) Physiochemical and environmental plant physiology, 4th edn. Academic press, Amsterdam 582

Olivo N, Girona J, Marsal J (2009) Seasonal sensitivity of stem water potential to vapour pressure deficit in grapevine. Irrig Sci 27(2):175–182

Poni S, Bernizzonia F, Civardia S, Gattia M, Porro D, Caminc F (2009) Performance and water-use efficiency (single-leaf vs. whole-canopy) of well-watered and half-stressed split-root Lambrusco grapevines grown in Po Valley (Italy). Agric Ecosyst Environ 129:97–106

Pou A, Medrano H, Tomàs M, Martorell S, Ribas-Carbó M, Flexas J (2012) Anisohydric behaviour in grapevines results in better performance under moderate water stress and recovery than isohydric behaviour. Plant Soil 359:335–349

Rogiers SY, Greer DH, Hatfield JM, Hutton RJ, Clarke SJ, Hutchinson PA, Somers A (2012) Stomatal response of an anisohydric grapevine cultivar to evaporative demand, available soil moisture and abscisic acid. Tree Physiol 32(3):249–261

SAS (2002) Enterprise guide version 42. SAS Institute Inc., Cary

Schultz HR (2003) Differences in hydraulic architecture account for near-isohydric and anisohydric behavior of two field-grown *Vitis vinifera* L. cultivars during drought. Plant Cell Environ 26(8):1393–1405

Schultz HR, Stoll M (2010) Some critical issues in environmental physiology of grapevines: future challenges and current limitations. Aust J Grape Wine Res 16:4–24

Sepulcre-Canto G, Zarco-Tejada PJ, Jimenez-Muñoz JC, Sobrino JA, de Miguel E, Villalobos FJ (2006) Detection of water stress in an olive orchard with thermal remote sensing imagery. Agric For Meteo 136:31–44

Soar CJ, Dry PR, Loveys BR (2006a) Scion photosynthesis and leaf gas exchange in *Vitis vinifera* L. cv. Shiraz: mediation of rootstock effects via xylem sap ABA. Aust J Grape Wine Res 12:82–96

Soar CJ, Speirs J, Maffei SM, Penrose AB, McCarthy MG, Loveys BR (2006b) Grape vine varieties Shiraz and Grenache differ in their stomatal response to VPD: apparent links with ABA physiology and gene expression in leaf tissue. Aust J Grape Wine Res 12:2–12

Tardieu F, Davies WJ (1993) Integration of hydraulic and chemical signalling in the control of stomatal conductance and water status of droughted plants. Plant Cell Environ 16(4):341–349

Testi L, Goldhamer DA, Iniesta F, Salinas M (2008) Crop water stress index is a sensitive water stress indicator in pistachio trees. Irrig Sci 26(5):395–405

Turner NC, Long MJ (1980) Errors arising from rapid water loss in the measurement of leaf water potential by pressure chamber technique. Aust J Plant Physiol 7(5):527–537

Weathon AD, Cooley NC, Dunn GM (2011) Use of thermal imagery to detect water stress during berry ripening in *Vitis vinifera* L. 'Cabernet sauvignon'. In: 6th IS on irrigation of Hort Crops Acta Hort 889:123–130

Weyers JDB, Meidner H (1990) Methods in stomatal research. Longman Scientific & Technical, Harlow

Williams LE, Araujo FJ (2002) Correlations among predawn leaf, midday leaf and midday stem water potential and their correlations with other measures of soil and plant water status in *Vitis vinifera*. J Am Soc Hort Sci 127(3):448–454

Yuan G, Luo Y, Sun X, Tang D (2004) Evaluation of a crop water stress index for detecting water stress in winter wheat in the North China Plain. Agric Water Manag 64(1):29–40